Neural Circuitry in Response to Reward and Loss in Females Exposed to Early Life Stress

Psych 204b Class Project
Joshua Jun Hwan Ryu; jhryu25@stanford.edu
Lauren Rebekah Borchers; lrborchers@stanford.edu
2019/06/06

Introduction

Exposure to trauma and stress in early life is associated with a variety of adverse behavioral outcomes, such as poor social functioning (Bolger & Patterson, 2001), higher depressive and anxious symptomatology (Gatt et al., 2009), and increased substance use dependence (Enoch, 2011). In addition, early life stress has also been associated with smaller volume of the amygdala and hippocampus (Gatt et al., 2009) and differing functional activation in the amygdala (Suzuki et al., 2014).

Due to the widespread effect on behavioral functioning and brain structure and function, understanding the neural mechanisms underlying early life stress is of critical importance. In this study, we sought to investigate the role between the bilateral nucleus accumbens and amygdala in relation to reward and loss. The nucleus accumbens is located in the basal forebrain and has been implicated in reward circuitry (e.g. Knutson et al., 2001). The amygdala is located in the frontal area of the temporal lobe and has been implicated in fear and arousal (e.g. Suzuki et al., 2014). Due to the role of the nucleus accumbens and the amygdala, we sought to determine the hemodynamic response in female adolescents exposed to low and high levels of early life stress in response to the anticipation of reward or loss. Demographic characteristics of the sample are reported in Table 1.

Hypothesis 1: Activation in the bilateral nucleus accumbens will increase during the anticipation of reward.

1.1: Activation in the bilateral nucleus accumbens will be greater for female participants exposed to *lower* levels of early life stress.

Hypothesis 2: Activation in the amygdala will increase during the anticipation of loss.

2.2: Activation in the amygdala will be greater for female participants exposed to *higher* levels of early life stress.

Exploratory analysis: We will also assess the beta weights for all regions of interest identified in FreeSurfer to determine whether other regions of the brain are activated during the functional task and whether the bilateral nucleus accumbens or amygdala coactivate with other regions in the brain.

Methods

Behavioral measure

Early life stress was measured using the Traumatic Events Screening Inventory for Children (TESI-C) (children reported on stressful life events and indicated how much it impacted them). A panel of coders then rated the objective severity of the stressful experience using the University of California Los Angeles Life Stress Interview coding system (Rudolph and Hammen, 1999; Rudolph et al., 2000). This allowed us to measure both subjective and objective stress. Each stressful life event was scored from zero to four, zero indicating a non-event with no impact and a four indicating severe event or impact. We focused on the sum of the severity for each stressful event the child experienced.

Functional Task

We implemented the Monetary Incentive Delay task for Children (KIDMID), a functional task that measures the anticipation of gain and loss, actual gain and loss, in addition to neutral stimuli (Figure 1). The KIDMID consists of one hundred six-second trials in which participants can win points if they hit a target quickly enough (total scan lasts approximately 8 minutes). The task consists of an anticipatory period (anticipation of gain or anticipation of loss) in which participants receive a cue (circle, square, or triangle). A circle indicates that the participant can win points, a square indicates a participant can avoid losing points, and the triangle indicates that the participant should not respond at all (similar to that of a go no go task). Participants were notified of how many points they could win or lose as indicated by lines in the circle or square (1 line = +/- 1 point; 2 lines = +/- 5 points). Then, participants received feedback regarding whether they had won or lost points (outcome gain or loss).

Anticipation of reward and loss followed by feedback and neutral stimuli were randomly presented for each participant.

Data Acquisition

All scans were collected at the Center for Cognitive and Neurobiological Imaging at Stanford on a 3.0 Tesla FE MRI scanner using a 32 head-channel coil (https://cni.stanford.edu).

We acquired a high-resolution anatomical T1-weighted image. The parameters for the T1-weighted SPGR image are as follows: frequency Rx direction=S/I sagittal; field of view=230x230; TR=0.00624; voxel dimensions = 3.2x3.2x3.0 mm^3. The duration of the T1-weighted image was 5 minutes and 15 seconds.

The parameters for the functional KIDMID task are as follows: slice thickness=3; number of slices=43; the frequency of the Rx direction is R/L oblique (AC-PC), the phases=250; field of view=224x224, and the TR=2. The duration of the KIDMID was 8 minutes and 20 seconds.

Preprocessing

We preprocessed and analyzed the functional MRI data in individual subject space (Figure 2). We first aligned all the functional images of a run to the mean of the functional images using rigid body transforms in SPM (http://www.fil.ion.ucl.ac.uk/spm/). The functional

mean images were then coregistered to T1-weighted SPGR anatomical image in SPM. Finally, we segmented the anatomical image and extracted the regions of interest, including the nucleus accumbens and amygdala in FreeSurfer (http://surfer.nmr.mgh.harvard.edu/).

Regions of interest

A priori, we were interested in investigating the bilateral nucleus accumbens and amygdala due to their role in reward and emotion (Figures 3 and 4). We segmented these regions of interest from a T1-weighted SPGR image in each participant using FreeSurfer (e.g. Dale et al., 1999; Dale and Sereno, 1993; Fischl and Dale, 2000). We segmented cortical regions (aparc in FreeSurfer) using a probabilistic atlas in Desikan et al., 2006 and subcortical regions (aseg in FreeSurfer) using subcortical segmentations given in Fischl et al., 2002.

Timecourses (Figure 6) for each voxel were extracted from the coregistered functional images and converted to percent change signals relative to the average signal for the entire run of the given voxel. Then, the timecourses were averaged within each of the segmented regions to obtain the timecourses in the corresponding region of interest.

General linear model

Using the SPM hrf, we conducted a series of general linear models (Figure 8) controlling for variation accounted for by movement of the participant (in the x-y-z planes as well as in the pitch, roll, and yaw axes). We began by fitting the model for every voxel in the brain so that we derived a beta value for each voxel. We then calculated an average beta for each region of interest by averaging all of the beta voxels in the corresponding region.

Once the mean beta values for each region of interest from the model were calculated, we conducted independent-samples t-tests, two-sided comparing the task conditions (e.g. anticipation of gain and anticipation of loss compared to neutral) as well as the two different groups (high versus low early life stress). In line with common practice, we thresholded the t statistics at $t = 2.0$ (approximate p value = .023) in order to focus on signals with a significant increase or decrease in the hemodynamic response.

Functional connectivity analyses

Finally, we assessed whether changes in the hemodynamic response were coactivated with other regions in the brain. That is, we assessed whether an increase or decrease in the hemodynamic response in the nucleus accumbens was associated with an increase or decrease in the hemodynamic response of the amygdala during the anticipation of gain (Cauda et al., 2011).

For the connectivity analyses we correlated three different timecourses: (1) raw percent change time course, (2) task related signals, and (3) background activity. The average percent change timecourse of each of the region was used as the raw percent change time course. The task-related signal was the task condition parameters multiplied by their respective beta weights. This removed the unexplained signal and the motion related signals from the timecourse. The background activity was defined as the error of the GLM model. Two connectivity measures were used, using pearson correlation of: (1) the signal and (2) the temporal derivatives of the signal (Shine et al. 2015). In the scope of this paper, we show the pearson correlations of the task-related signals.

*All of the codes, sparsely annotated, for the analysis can be found at: https://github.com/joshryu0425/ELSstudy.git

Results

General linear model contrasts

We conducted general linear models to assess the model fit for our regions of interest, controlling for motion in the x-y-z planes as well as the pitch, roll, and yaw axes using the SPM hrf. Generally, the general linear models did a good job of explaining variance in our regions of interest. We looked at the beta-value contrasts comparing the anticipation of gain or loss compared to the neutral condition for each participant (Figures 4,5). We then conducted a two sample t-test of the beta contrasts for the low early life stress versus the high early life stress samples (Figure 9,10). Independent-samples t-tests revealed no significant differences for anticipation of reward in the left nucleus accumbens ($t(7)=0.76$, $p=.471$) or right nucleus accumbens ($t(7)=0.71$, $p=.498$). Further, there were no significant differences between the anticipation of loss in the left amygdala $t(7)=1.75$, $p=.123$) or right amygdala $t(7)=0.17$, $p=.868$)

Functional Connectivity

The whole brain functional connectivity between the regions of interest from the aparc and aseg segmentation were assessed visually (Figure 11). There was a high correlation between nearby regions of interest, including high functional connectivity within the reward circuitry. The cortex in general was negatively correlated with regions of the default mode network (indicated by blue columns and rows). The right hemisphere was also highly correlated with the corresponding anatomical regions in the left hemisphere (indicated by yellow columns and rows).

We looked at functional connectivity between regions of interest specifically, the bilateral nucleus accumbens and the amygdala (Figure 12). Generally, we saw that as activation increased in one region of the brain, other regions were activated as well. When we looked at the connectivity between groups we found that participants exposed to low levels of early life stress showed significantly more coactivation between the left amygdala and the nucleus accumbens compared to participants exposed to high levels of early life stress (Figure 13; Table 2).

Conclusions

Summary

In sum, we did not detect any significant between-group differences in activation of the left or right nucleus accumbens in anticipation of reward or in the left and right amygdala in the anticipation of loss. Additional analyses revealed differences in functional connectivity between regions of interest. Specifically, participants in the low early life stress group showed more

functional connectivity between these regions of interest compared to the high early life stress group.

Limitations

The main limitation of the current study is the small sample size, for the scope of the analysis. Further, we limited all analyses to female participants exposed to low levels of early life stress or very high levels of early life stress, thus not encompassing a representative sample. The timecourse plot (Figure 6) and the statistical maps (Figures 4, 5) of the contrast showed signal but also a lot of variability within the voxels and across voxels within the regions of interest. For example, we saw activation in the white matter of the brain which is indicative of high measurement noise and associated false positive rate. A source of variability comes from the small trial number. Each subject had one run of about 8 minutes, and with 6 second blocks for each condition (7 conditions: 3 loss, 3 gains, and 1 neutral), giving us about 10 trials per condition. There may not have been enough trials to assess the differential effects of each condition. Furthermore, with the relatively long TR of 2 seconds and the small amount of time between stimuli, the signals from the cue, target, and feedback are likely to have been intermixed at a given time. A source of within region variation may have been from the poor region of interest definition. This could be due to poor segmentation, which would not be surprising given that we used probabilistic segmentation created for adults in adolescents. The problem may be mitigated with better parcellation or the use of functionally derived regions of interest from other runs of the dataset.

The general linear model also has several limitations. The histograms of the beta values showed that some voxels had physiologically unrealistic beta values (Figure 7). The problem of ill-conditioned regression can be mitigated by use of sparsity constraints, for instance, by using ridge regression. The regression can also be improved with a better model for the noise covariance matrix, such as taking into account temporal autocorrelations. Furthermore, the regression may benefit from a more accurate model of the hemodynamic response function, which may differ across the brain.

Future directions

Future work will assess whether the lack of group differences between the anticipation of gain and loss persist in a larger sample. This study assessed 228 individuals exposed to varying degrees of early life stress. Further work will also include male participants and assess early life stress along a continuum rather than as a categorical variable. In terms of the analysis, we plan to improve our segmentation, which may be achieved by manually drawing our regions of interest, by using different parcellations, or by using functionally defined regions of interest through principal components analysis. Furthermore, the general linear model can be also be improved by using ridge regression.

Figures and Tables

Figure 1. Example of the KIDMID task (task created by Knutson et al., 2000; figure from Maresh, Allen, & Coan, 2014).

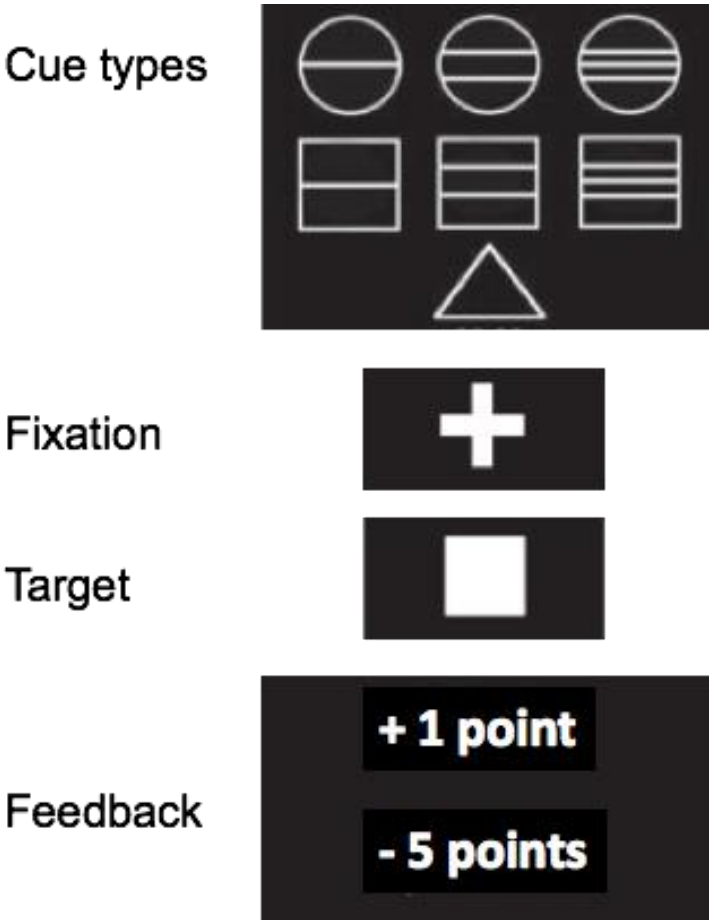

Figure 2: Analysis pipeline.

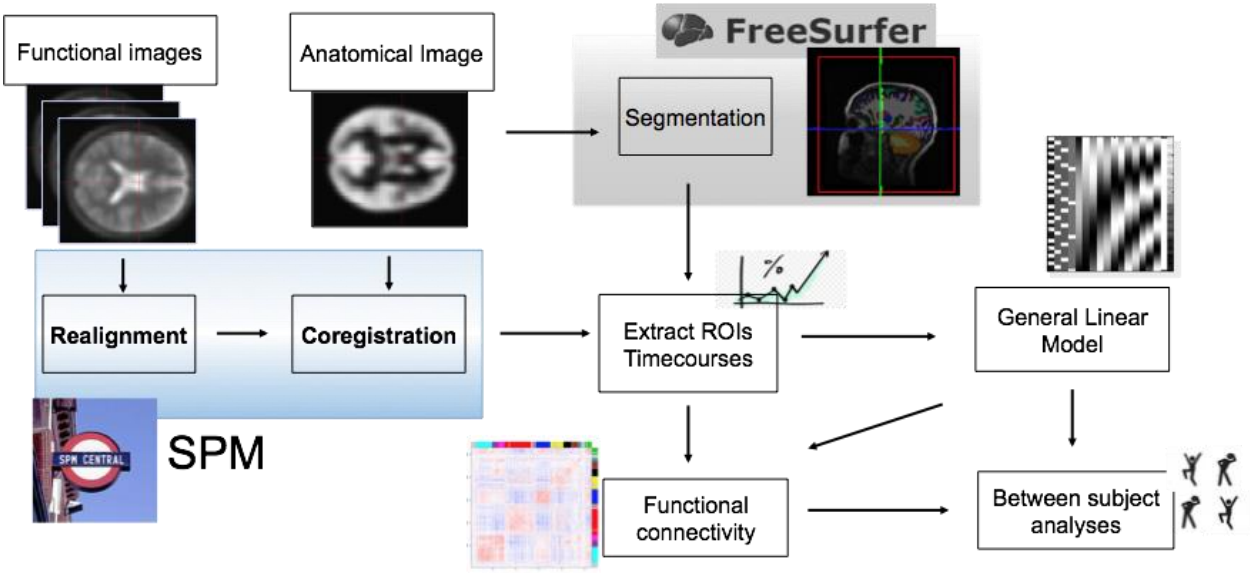

Figure 3. Regions of interest (left panel (nucleus accumbens) right panel (amygdala)).

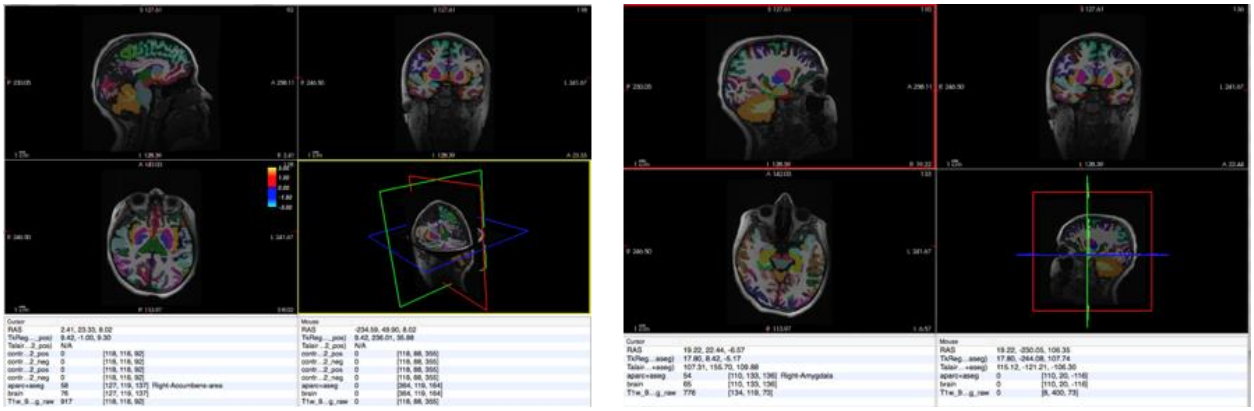

Figure 4. Nucleus accumbens (right) activation. Beta contrast = beta anticipation of gain - beta anticipation of neutral, plotted in one representative participant. T-values thresholded at $t = 2$.

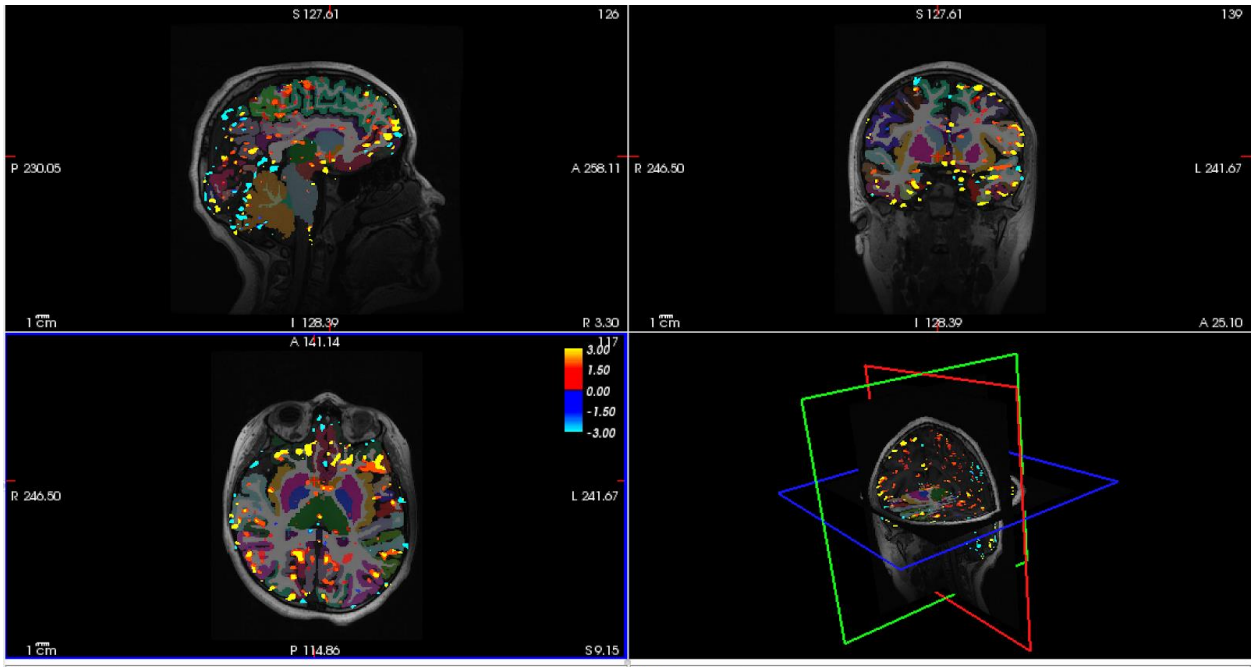

Cursor		
RAS	3.30, 25.10, 9.15	
TkReg…aseg)	1.88, 11.07, 10.54	
Talair…+aseg)	123.02, 138.29, 123.46	
contr…2_pos	0	[116, 116, 91]
contr…2_neg	0	[116, 116, 91]
contr…2_pos	0	[116, 116, 91]
contr…2_neg	0	[116, 116, 91]
contr…2_pos	0	[116, 116, 91]
contr…2_neg	0	[116, 116, 91]
aparc+aseg	58	[126, 117, 139] Right-Accumbens-area
brain	77	[126, 117, 139]
T1w_9…g_raw	950	[116, 116, 91]

Mouse		
RAS	-192.15, -28.05, 9.15	
TkReg…aseg)	-193.56, -42.07, 10.54	
Talair…+aseg)	336.96, 102.96, 96.35	
contr…2_pos	0	[116, 175, 308]
contr…2_neg	0	[116, 175, 308]
contr…2_pos	0	[116, 175, 308]
contr…2_neg	0	[116, 175, 308]
contr…2_pos	0	[116, 175, 308]
contr…2_neg	0	[116, 175, 308]
aparc+aseg	0	[322, 117, 86]
brain	0	[322, 117, 86]
T1w_9…g_raw	0	[116, 175, 308]

Figure 5. Amygdala (left) activation. Beta contrast = beta anticipation of loss - beta anticipation of neutral, plotted in one representative participant. T-values thresholded at $t = 2$.

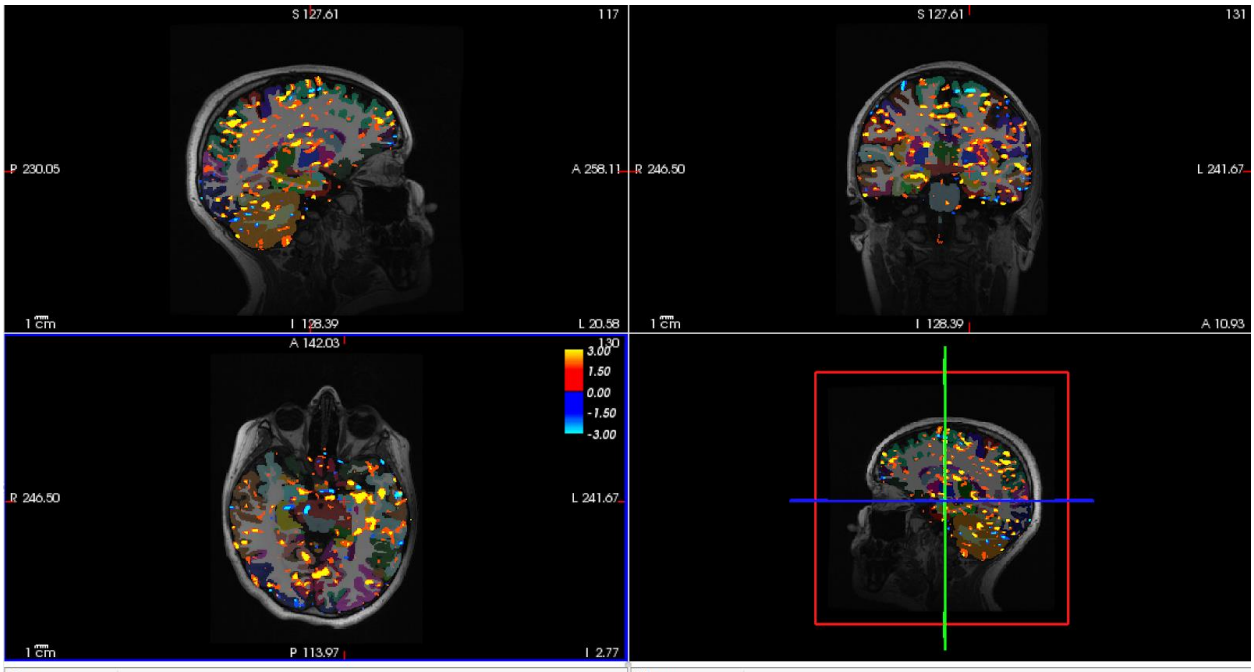

Cursor		
RAS	-20.58, 10.93, -2.77	
TkReg…_pos)	-1.37, 21.99, -3.10	
Talair…2_pos)	N/A	
contr…2_pos	0	[130, 131, 117]
contr…2_neg	0	[130, 131, 117]
contr…2_pos	0	[130, 131, 117]
contr…2_neg	0	[130, 131, 117]
aparc+aseg	18	[150, 129, 125] Left-Amygdala
brain	72	[150, 129, 125]
T1w_9…g_raw	781	[130, 131, 117]

Mouse		
RAS	-162.96, -102.46, -2.77	
TkReg…_pos)	-1.37, 164.37, -116.48	
Talair…2_pos)	N/A	
contr…2_pos	0	[130, 258, 276]
contr…2_neg	0	[130, 258, 276]
contr…2_pos	0	[130, 258, 276]
contr…2_neg	0	[130, 258, 276]
aparc+aseg	0	[292, 129, 12]
brain	0	[292, 129, 12]
T1w_9…g_raw	0	[130, 258, 276]

Figure 6. Percent change timecourse in the left amygdala plotted in one representative participant.

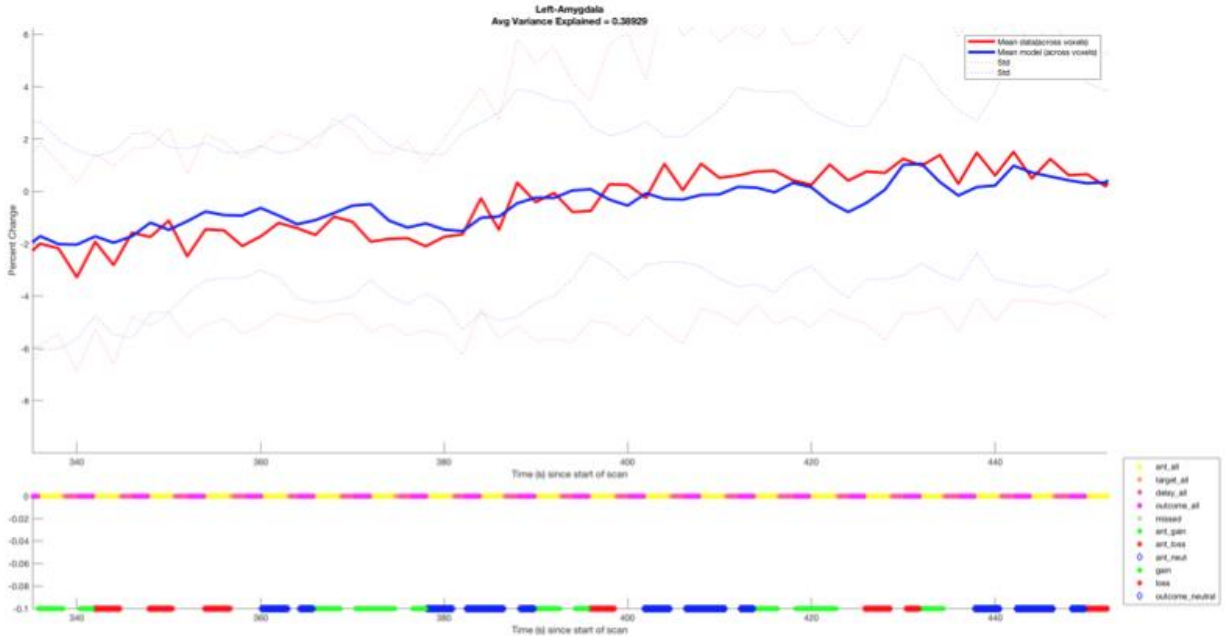

Figure 7. Histograms for the distribution of beta weights and R^2 values in the left amygdala, for one representative participant. Top left: anticipation of gain; top right: anticipation of loss; bottom left: anticipation of neutral; bottom right: R^2 values.

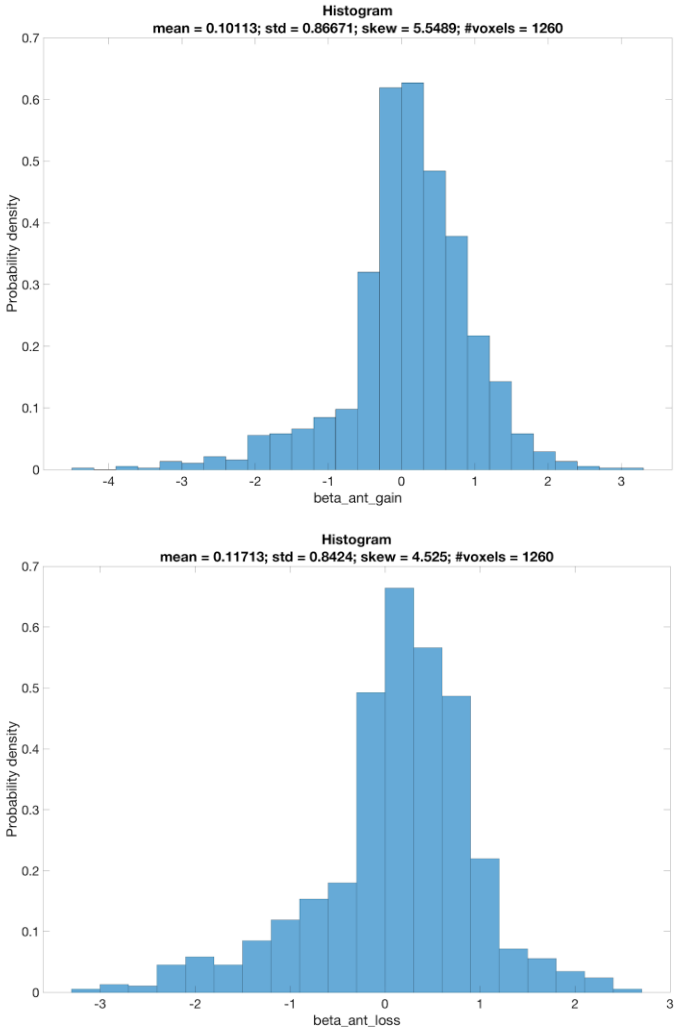

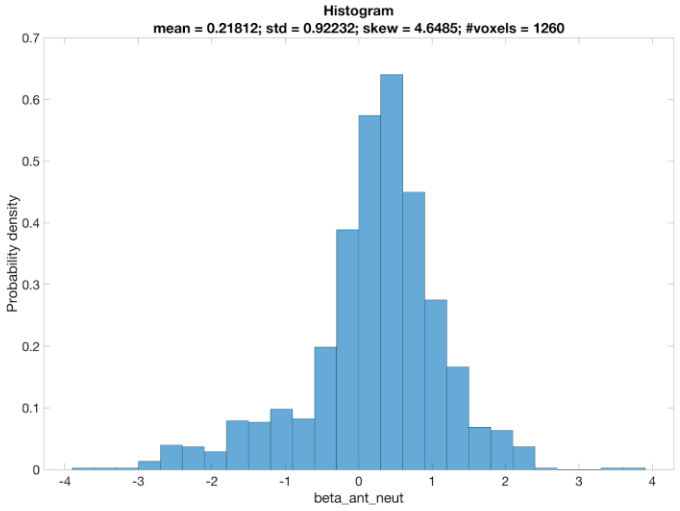
Histogram
mean = 0.21812; std = 0.92232; skew = 4.6485; #voxels = 1260
Probability density
beta_ant_neut

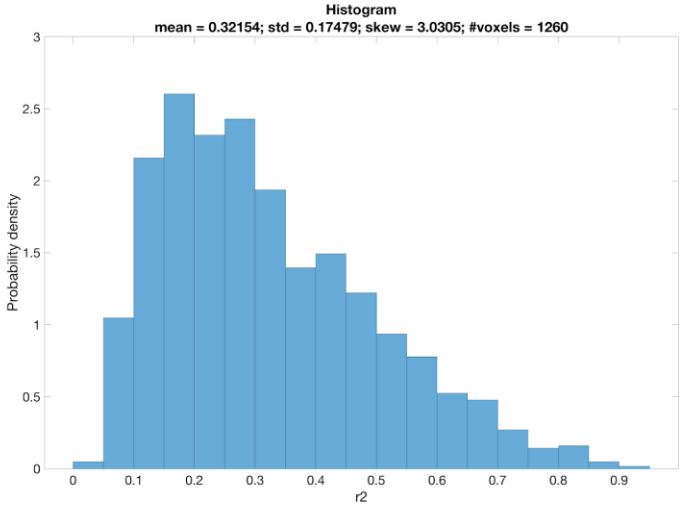
Histogram
mean = 0.32154; std = 0.17479; skew = 3.0305; #voxels = 1260
Probability density
r2

Figure 8. General linear model design matrix in one representative participant (left-hand side are the different conditions in the KIDMID, right-hand side are covariates of interest related to motion), plotted in one representative participant.

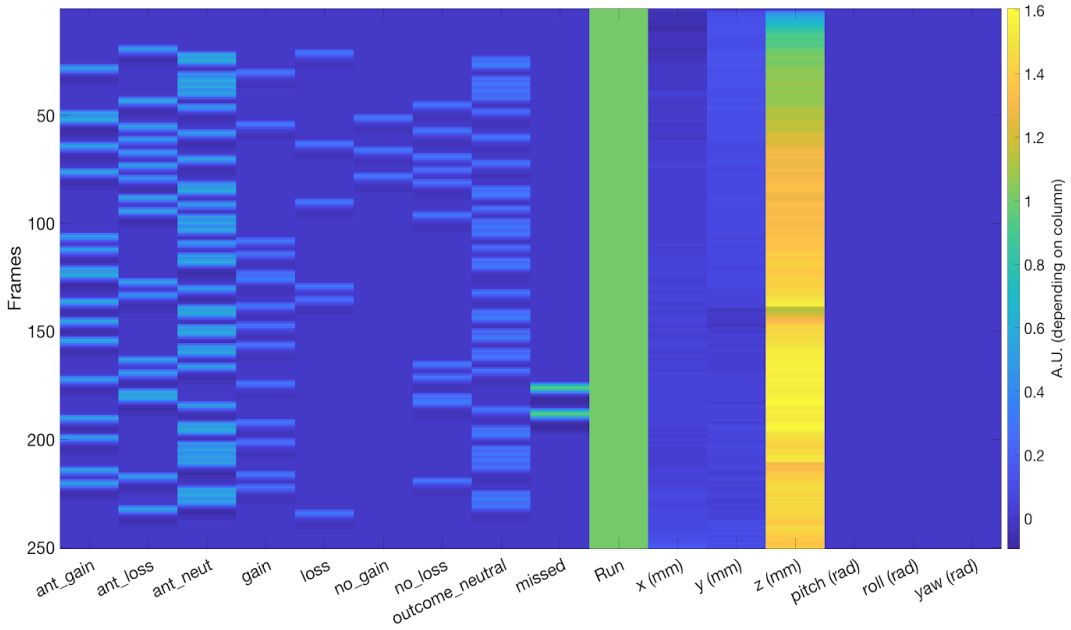

Figure 9. Anticipation of reward in the left and right nucleus accumbens (low early life stress (ELS) plotted in blue; high ELS plotted in orange).

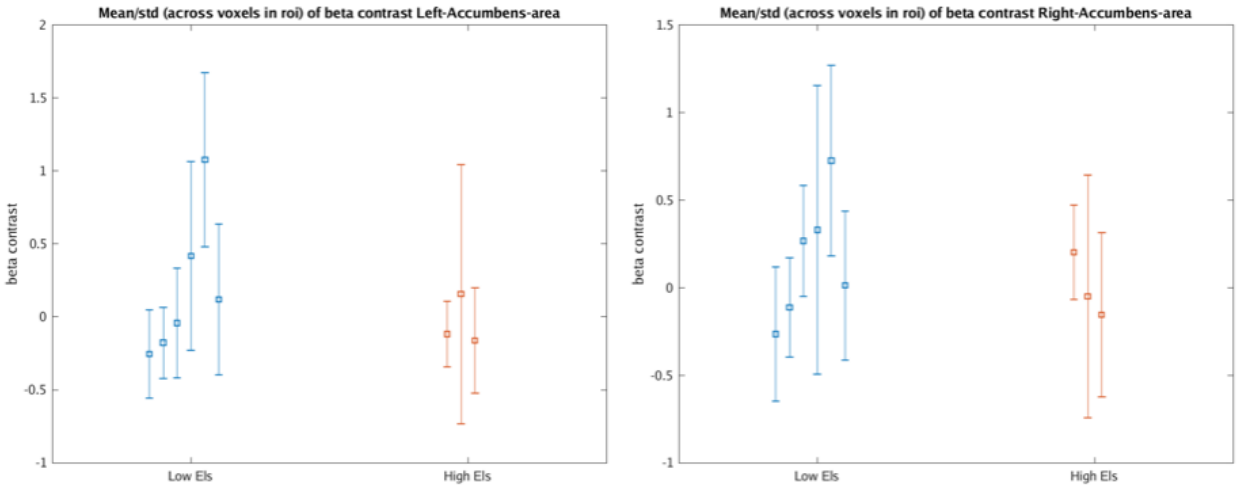

Figure 10. Anticipation of loss in the left and right amygdala (low early life stress (ELS) plotted in blue; high ELS plotted in orange).

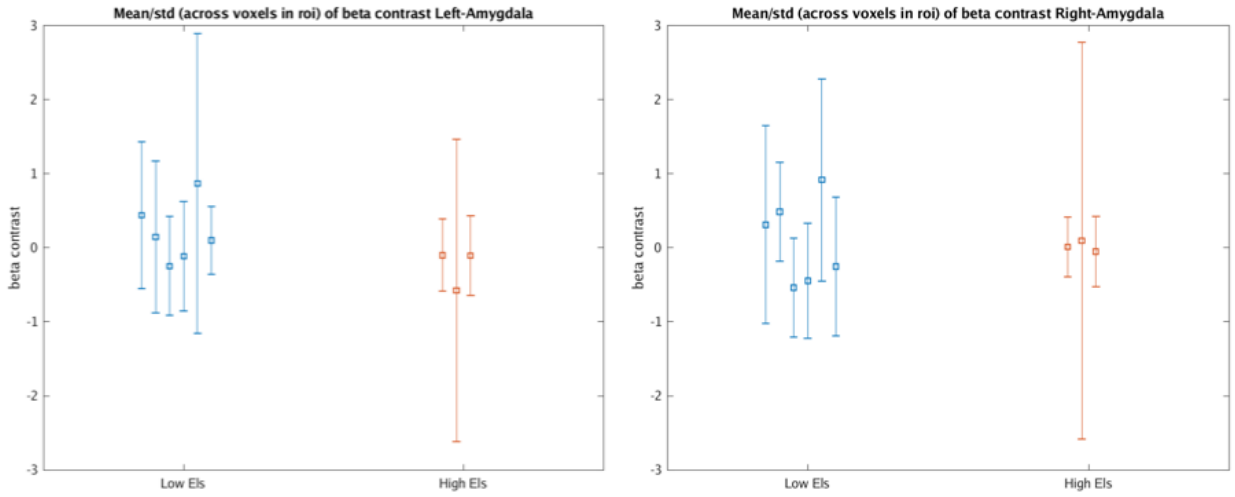

Figure 11. Coactivation matrix showing all regions in the brain for a sample participant.

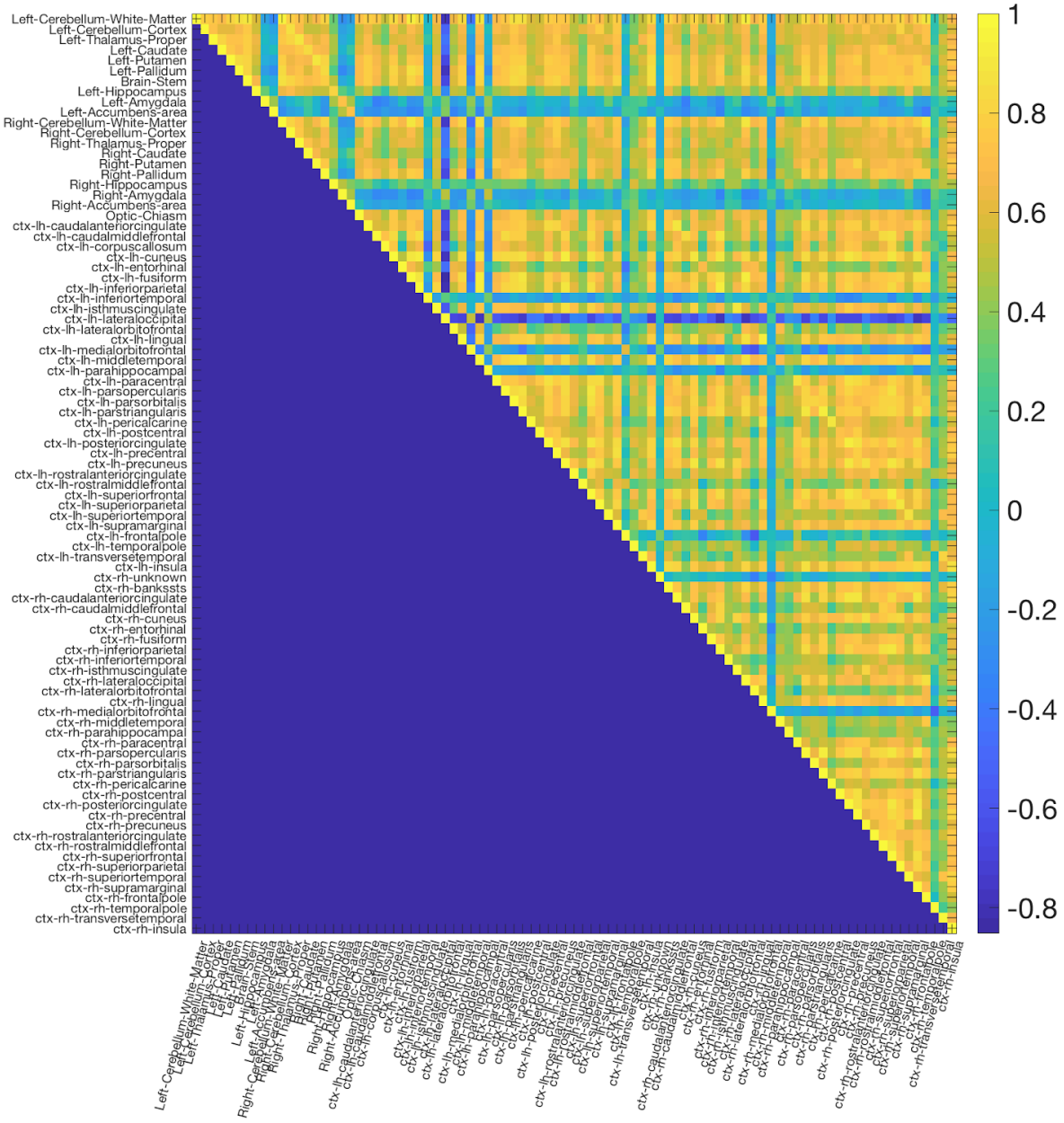

Figure 12. Coactivation matrix in regions of interest in a representative participant.

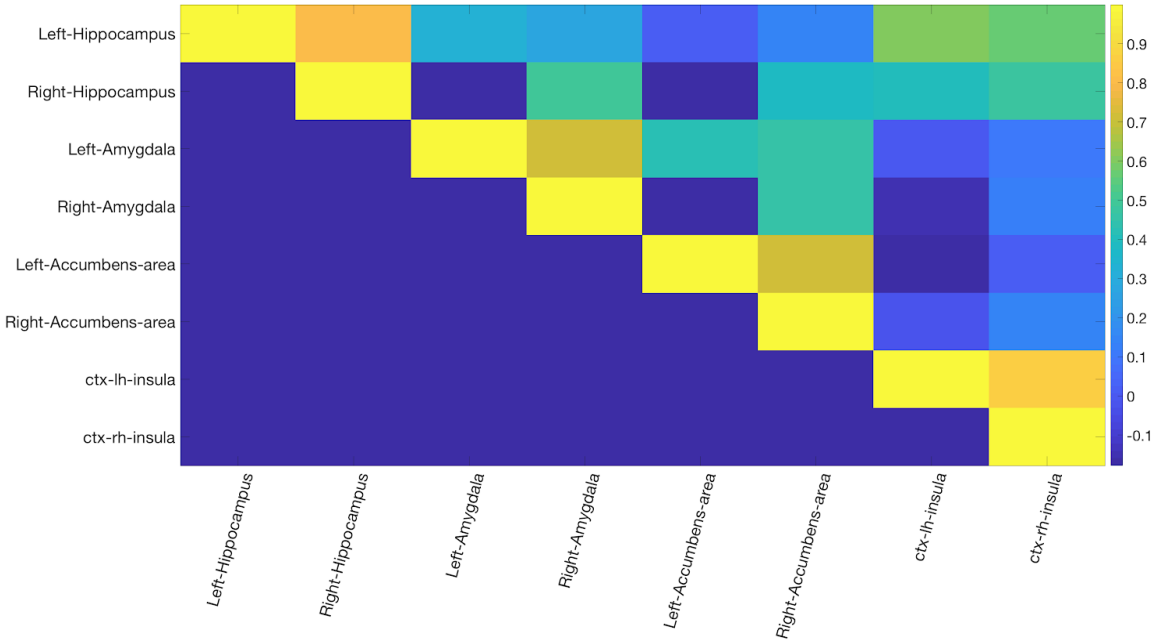

Figure 13. Coactivation matrix in regions of interest in participants with low early life stress (ELS) (green) compared to high ELS (red).

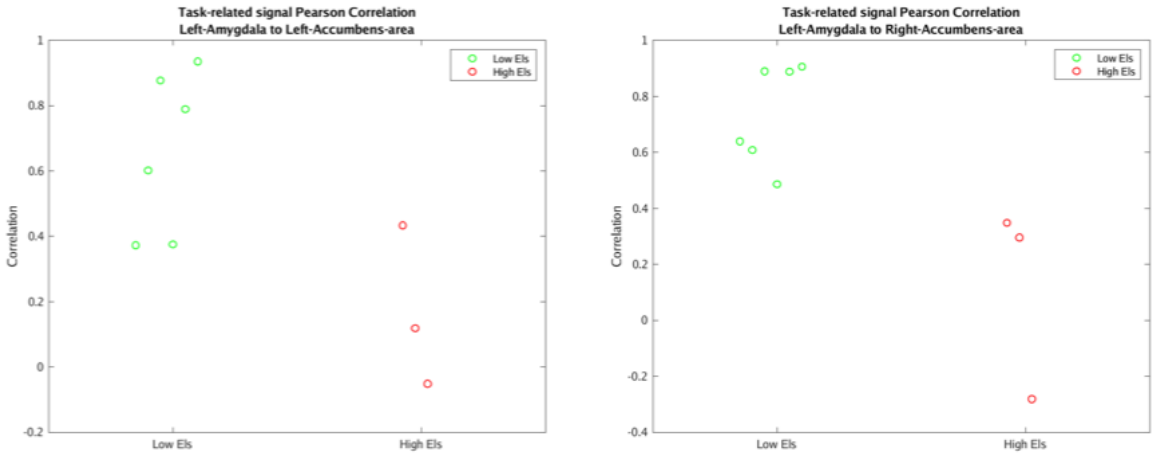

Table 1: Demographic characteristics of the sample.

Total sample; *N* = 9	Low ELS (*n* = 6)	High ELS (*n* = 3)	*t*	*p*
Age (at scan; years)	10.98	11.47	-0.56	.591
Body mass index	17.55	25.46	-2.14	.069
Tanner Stage (avg)	2.25	3.00	-1.66	.142
Early life stress	0.92	15.67	**-10.74**	**.008**

Tanner Stage is an index of pubertal development.
Early life stress (ELS) was measured with the TESI-C (see above).

Table 2: T-tests for task-related connectivity.

High vs. low ELS	Right NAcc	Left Amygdala	Right Amygdala
Left NAcc	*t*=1.71, *p*=.131	***t* =2.81, *p*=.026***	*t*=1.80, *p*=.114
Right NAcc	-	***t*=3.60, =.009****	*t*=1.96, *p*=.091
Left Amygdala	-	-	*t*=1.33, *p*=.226

ELS: Early life stress

df=7 for all t-tests

References

Bolger, K. E., & Patterson, C. J. (2001). Developmental pathways from child maltreatment to peer rejection. *Child development, 72*(2), 549-568.

Cauda, F., Cavanna, A. E., D'agata, F., Sacco, K., Duca, S., & Geminiani, G. C. (2011). Functional connectivity and coactivation of the nucleus accumbens: a combined functional connectivity and structure-based meta-analysis. *Journal of cognitive neuroscience*, *23*(10), 2864-2877.

Dale, A.M., Sereno, M.I., 1993. Improved localization of cortical activity by combining EEG and MEG with MRI cortical surface reconstruction: a linear approach. J Cogn Neurosci 5, 162-176

Dale, A.M., Fischl, B., Sereno, M.I., 1999. Cortical surface-based analysis. I. Segmentation and surface reconstruction. Neuroimage 9, 179-194.

Desikan, R. S., Ségonne, F., Fischl, B., Quinn, B. T., Dickerson, B. C., Blacker, D., ... & Albert, M. S. (2006). An automated labeling system for subdividing the human cerebral cortex on MRI scans into gyral based regions of interest. *Neuroimage*, *31*(3), 968-980.

Enoch, M. A. (2011). The role of early life stress as a predictor for alcohol and drug dependence. *Psychopharmacology, 214*(1), 17-31.

Fischl, B., Salat, D. H., Busa, E., Albert, M., Dieterich, M., Haselgrove, C., ... & Montillo, A. (2002). *Whole brain segmentation: automated labeling of neuroanatomical structures in the human brain. Neuron*, 33(3), 341-355.

Gatt, J. M., Nemeroff, C. B., Dobson-Stone, C., Paul, R. H., Bryant, R. A., Schofield, P. R., ... & Williams, L. M. (2009). Interactions between BDNF Val66Met polymorphism and early life stress predict brain and arousal pathways to syndromal depression and anxiety.

Molecular psychiatry, *14*(7), 681.

Ippen, C. G., Ford, J., Racusin, R., Acker, M., Bosquet, M., Rogers, K., Ellis, C., Schiffman, J., Ribbe, D.,Cone, P., Lukovitz, M., & Edwards, J. (2002). *Traumatic Events Screening Inventory - Parent Report Revised.*

Knutson B, Westdorp A, Kaiser E, Hommer D: FMRI visualization of brain activity during a monetary incentive delay task. Neuroimage 2000, 12:20–27.

Knutson, B., Adams, C. M., Fong, G. W., & Hommer, D. (2001). Anticipation of increasing monetary reward selectively recruits nucleus accumbens. *Journal of Neuroscience*, *21*(16), RC159-RC159.

Maresh, E. L., Allen, J. P., & Coan, J. A. (2014). Increased default mode network activity in socially anxious individuals during reward processing. *Biology of mood & anxiety disorders*, *4*(1), 7.

Ribbe, D. (1996). Psychometric review of Traumatic Event Screening Instrument for Children (TESI-C). In B. H. Stamm (Ed.), *Measurement of stress, trauma, and adaptation* (pp. 386-387). Lutherville, MD: Sidran Press.

Rudolph, K. D., & Hammen, C. (1999). Age and gender as determinants of stress exposure, generation, and reactions in youngsters: A transactional perspective. *Child development*, *70*(3), 660-677.

Rudolph, K. D., Hammen, C., Burge, D., Lindberg, N., Herzberg, D., & Daley, S. E. (2000). Toward an interpersonal life-stress model of depression: The developmental context of stress generation. *Development and psychopathology*, *12*(2), 215-234.

Shine, J. M., Koyejo, O., Bell, P. T., Gorgolewski, K. J., Gilat, M., & Poldrack, R. A. (2015). Estimation of dynamic functional connectivity using Multiplication of Temporal

Derivatives. *NeuroImage*, *122*, 399-407.

Suzuki, H., Luby, J. L., Botteron, K. N., Dietrich, R., McAvoy, M. P., & Barch, D. M. (2014). Early life stress and trauma and enhanced limbic activation to emotionally valenced faces in depressed and healthy children. *Journal of the American Academy of Child & Adolescent Psychiatry*, *53*(7), 800-813.